Removal of Lead and Copper Ions onto Granular Activated Carbon in Batch and Fixed Bed A Dsorber

Abbass H. Sulaymon[*], Balasim A. Abid[**] & Jenan A. Al Najar[**]

Rexeived on: 31/12/2008
Accepted on: 7/5/2009

Abstract

The adsorption of lead and copper ions onto granular activated carbon (DARCO 20-40 mesh) in a single component system has been studied using fixed bed adsorbers. A film-pore diffusion model has been developed to predict the fixed bed breakthrough curves for the two metal ions. This model takes account both external and internal mass transfer resistance as well as axial dispersion with non-linear isotherm. The effects of flow rate, bed height and initial metal ion concentration has been studied. Batch adsorber experiments were conducted to estimate the parameters required for fixed bed model, such as adsorption equilibrium isotherm constants the external mass transfer coefficient and pore diffusion coefficient by fitting the experimental data with theoretical model. The batch isotherm experimental data was correlated using Langmuir and Freundlich isotherm models. The adsorption isotherm data follow the Langmuir model better than Freundlich model. The pore diffusion coefficient was obtained using pore diffusion model for batch adsorber by matching between the experimental data and predicted data from the model. The results show that the film-pore diffusion model used for fixed bed adsorber provide a good description of the adsorption process for adsorption of metal ions Pb(II) and Cu(II) onto activated carbon in fixed bed adsorber.

Keywords: Removal; Heavy metals; Activated carbon; Batch adsorber; Fixed bed adsorber

ازالة الرصاص والنحاس باستخدام الكاربون المنشط الحبيبي بواسطة الامنزاز في عملية دفعية والامتزاز في عمود الحشوة الثابتة

الخلاصه

تم درسة ازالة الرصاص والنحاس بواسطة الامتزاز على الكاربون المنشط الحبيبي في عملية دفعية وفي عمود الحشوة الثابتة. في عملية الامتزاز باستخدام الحشوة الثابتة تم استنباط موديل رياضي لايجاد منحنيات الاختراق. الموديل ياخذ بنظر الاعتبار المقاومة الخارجية والمقاومة الداخلية لانتقال المادة وكذلك الانتشار المحوري مع استخدام معادلة غير خطية

لتمثيل حالة الاتزان لنظام ثابت الحرارة. تم اجراء الامتزاز في عملية دفعية لايجاد ثوابت الاتزان, معامل الانتقال الخارجي ومعامل الانتشار داخل الحبيبات من خلال مطابقة النتائج العملية مع النتائج المستحصلة من الموديل النظري. تم مطابقة النتائج العملية المستحصلة من تجربة الاتزان مع النتائج النظرية المستحصلة من عدد من علاقة الانزان لنظام ثابت الحرارة ووجد أن النتائج العملية تتبع معادلة لانكماير بصورة جيدة. معامل الانتشار الحبيبي تم

* Environment Engineering Department, College of Engineering, University of Baghdad/ Baghdad
**Chemical Engineering Department, University of Technology/ Beghdad

الحصول عليه من خلال مطابقة النتائج العملية في عملية دفعية مع النتـــائج المستحـــصلة مـــن الموديل الرياضي لعملية دفعية. النتائج العملية في تجربة الحشوة الثابتة اظهرت بـــان الموديـــل الرياضي المستخدم لتمثيل الامتزاز في الحشوة الثابتة يعطـــي وصـــفا جيـــد لعمليـــة امتـــزاز الرصاص والنحاس باستخدام الكاربون المنشط كحشوة ثابتة.

1. Introduction

Heavy metals are among the most toxic contaminants of surface water. The main sources of toxic metals are industrial wastes from processes such as electroplating, metal finishing, chemical manufacturing and nuclear fuel processing. Since most of heavy metals are non degradable into nontoxic metals end products, these concentration must be reduced to acceptable levels before discharged them into environment. Otherwise these could pose threat to public health and/or affect the quality of potable water [1]. Effect of metals and their compounds on humans, animals and plants, is quite varied. Human metal intake may occur primarily from contaminated food, drinking water, skin and lung adsorption. According to the World Health Organization [2] and International Programmed on Chemical Safety [3], the most toxic metals are aluminum, chromium, magnesium, iron, cobalt, nickel, copper, zinc, cadmium, mercury and lead.

Adsorption is found to be the most effective method for removing dissolved metal ions from wastes [1] . Adsorption is the most commonly used process because it is fairly simple and convenient unit operation and that the cost for its application is relatively low compared to other treatment processes. Adsorption by activated carbon has been widely studied as an effective technique for removing heavy metal from aqueous solution and wastewater.

For industrial applications in the waste water treatment, the most efficient arrangement for conducting adsorption operation is the fixed bed adsorber. The kinetics behavior of fixed-bed adsorber can be explained and the characteristic breakthrough curve of the adsorption phenomenon can be obtained through mathematical models. A number of mathematical models have been developed to explain the kinetic behavior of the fixed-bed adsorber and to estimate the breakthrough curve [4,5]. The mechanism of adsorption onto an adsorbent includes external diffusion, internal diffusion and adsorption.

In the present study, film-pore diffusion model is used to determine the breakthrough curves in fixed bed column for single component adsorption onto granular activated carbon and compare the experimental results

with that simulated by numerical simulation of the film-pore diffusion model, which includes film mass transfer and internal mass transfer resistance as well as axial dispersion with non linear isotherms.

2. Mathematical Model

Film-pore diffusion model is proposed to predict the fixed-bed breakthrough curves for single metal ion adsorbed onto porous media. The mathematical model takes account of: External mass transfer resistance, Internal mass transfer resistance, Non-ideal plug flow and Non-linear isotherm [5,6].

The following basic assumptions are made to formulate the pore diffusion model:

- The system operates under isothermal conditions.
- The equilibrium of the adsorption is described by Langmuir isotherm.
- Solid particles are spherical, uniform in size and density. They also do not swell or shrink.
- No radial concentration gradient in the column and no angular concentration gradient within a particle.
- The intraparticle mass transfer is due to Fickian diffusion and it is characterized by the constant pore diffusion coefficient, Dp.
- Mass transfer across the boundary layer surrounding the solid particles is characterized by the external film mass transfer coefficient kf .
- All the mechanisms which contribute to axial mixing are lumped together into a single axial dispersion coefficient.

Continuity equation in the bulk-fluid phase:

$$-D_L\frac{\partial^2 C_b}{\partial Z^2}+v\frac{\partial C_b}{\partial Z}+\frac{\partial C_b}{\partial t}+r_p\left(\frac{1-e_b}{e_b}\right)\frac{\partial q}{\partial t}=0 \quad \ldots(1)$$

The following initial and boundary conditions are considered:

$$\text{I.C.:}\quad C_b = C_{bo} \qquad Z = 0, t = 0 \quad \ldots.(2)$$

$$C_b = 0 \qquad 0 < Z \le L,\ t = 0 \quad \ldots.(3)$$

$$\text{B.C.:}\quad D_L\frac{\partial C_b}{\partial Z} = -v(C_{bo} - C_b) \qquad Z = 0,\ t > 0 \quad \ldots.(4)$$

$$\frac{\partial C_b}{\partial Z} = 0 \qquad Z = L,\ t \ge 0 \quad \ldots(5)$$

Using C_b the concentration in the stagnant fluid inside the macropore, the inter-phase mass transfer rate may be expressed as:

$$r_p\frac{\partial q}{\partial t} = \frac{3k_f}{R_p}(C_b - C_{p,R=R_p}) \quad \ldots.(6)$$

Substituting the term $\partial q/\partial t$ in equation 6 onto equation 1 gives:

$$-D_L\frac{\partial^2 C_b}{\partial Z^2}+v\frac{\partial C_b}{\partial Z}+\frac{\partial C_b}{\partial t}+\frac{3k_f(1-e_b)}{e_b R_p}(C_b-C_{p,R=R_p})=0$$

…. (7)

The particle phase continuity equation in spherical coordinates is as follows:

$$e_p\frac{\partial C_p}{\partial t}+(1-e_p)r_p\frac{\partial q}{\partial t}-e_p D_p\left(\frac{\partial^2 C_p}{\partial R^2}+\frac{2}{R}\frac{\partial C_p}{\partial R}\right)=0$$

….(8)

The following initial and boundary conditions are considered:

I.C.: $C_p = 0, q = 0$ $R = 0, t = 0$ …(9)

B.C.: $\frac{\partial C_p}{\partial R}=0,$ $R= 0, t > 0$ ..(10)

$$D_p\frac{\partial C_p}{\partial R}=k_f(C_b-C_{P,R=Rp})$$ $R=R_p, t\geq 0$ …(11)

Since equilibrium is assumed for adsorption at the interior site, q and C_p in equation 8 are related by the instantaneous equilibrium expression

$$\frac{\partial q}{\partial t}=\frac{\partial q}{\partial C_p}\frac{\partial C_p}{\partial t}$$

…(12)

Using equation 12 with equation 8 and rearranging of equation 8 yields:

$$\frac{\partial C_p}{\partial t}=\frac{1}{\left[1+r_p\left(\frac{1-e_p}{e_p}\right)\frac{\partial q}{\partial C_p}\right]}D_p\left(\frac{\partial^2 C_p}{\partial R^2}+\frac{2}{R}\frac{\partial C_p}{\partial R}\right)$$

….(13)

The adsorption isotherm is non-linear and described by Langmuir isotherm model:

$$q=\frac{q_m bC_p}{1+bC_p}$$

….(14)

Defining the following dimensionless variables:

$$c_b=\frac{C_b}{C_o},\ c_p=\frac{C_p}{C_o},\qquad q^{\bullet}=\frac{r_p q}{C_o},$$

$$t=\frac{nt}{L},\quad r=\frac{R}{R_p},\quad z=\frac{Z}{L}$$

The dimensionless parameters are defined as:

$$pe=\frac{nL}{D_L},\quad Bi=\frac{k_f R_p}{e_p D_p},\quad h=\frac{e_p D_p L}{R_p^2 n},$$

$$z=\frac{3Bi\,h\,(1-e_b)}{e_b}$$

The model equation 7 and the initial and boundary conditions, equations 2-5, can be transformed into the following dimensionless equations:

$$-\frac{1}{pe}\frac{\partial^2 c_b}{\partial z^2}+\frac{\partial c_b}{\partial z}+\frac{\partial c_b}{\partial t}+z\,(c_b-c_{p,r=1})=0$$

…. (15)

I.C.: $c_b = 1$ $z = 0, \tau = 0$ .....(16)

$c_b = 0$ $0 < z \leq 1, \tau = 0$ ....(17)

B.C.: $\frac{\partial c_b}{\partial z} = -pe(1-c_b)$ $z = 0, \tau > 0$ ....(18)

$\frac{\partial c_b}{\partial z} = 0$ $z = 1, \tau \geq 0$ ....(19)

The model equations 13 and the Langmuir equation 14 and the initial and boundary conditions, equations 9-11 can be transformed into the following dimensionless equations:

$$\frac{\partial c_p}{\partial t} = \frac{1}{\left[e_p + (1-e_p)\frac{\partial q^{\bullet}}{\partial c_p}\right]} h\left(\frac{\partial^2 c_p}{\partial r^2} + \frac{2}{r}\frac{\partial c_p}{\partial r}\right) \quad .....(20)$$

$$q^{\bullet} = \frac{r_p q_m b c_p}{1 + b c_p C_o} \quad ....(21)$$

I.C.: $c_p = 0,\ q^{\bullet} = 0$ $r = 0, \tau = 0$ ....(22)

B.C.: $\frac{\partial c_p}{\partial r} = 0$ $r = 0, \tau > 0$ .....(23)

$$\frac{\partial c_p}{\partial r} = Bi(c_b - c_{P,r=1}) \quad r = 1, \tau \geq 0 \quad .....(24)$$

Since non-linear adsorption equilibrium (Langmuir isotherm) is considered, the preceding set of partial differential equations 15-24 are solved numerically by reduction to set of ordinary differential equations using the Finite element method for the bulk-fluid partial differential equation and the orthogonal collocation method for the particle phase equations. The ordinary differential equation system with initial values can be readily solved using an ordinary differential equation solver such as the subroutine "ODE15S" OF MATLAB v.7 which is a variable order solver based on the numerical differentiation formulas (NDFs).

3. Experimental Work and Procedure

Adsorbate: 1000 mg/L standard stock solution of each metal ions of Pb(II) , Cu(II) were prepared by dissolving $Pb(No_3)_2$, $Cu(No_3)_2.3H_2O$ respectively in distilled water. The chemicals used are annular grade produced by Fluka and Aldrich-Sigma.

Adsorbent: The granular activated carbon (GAC) used was supplied by Sigma-Aldrich.Com., United Kingdom. Granular activated carbon was used directly without any treatment. The mean diameter of the GAC particles is 0.6 mm. The physical properties were measured by Thermochemistry Laboratory, Chemical Science

(FH&MS), University of Surrey, United Kingdom and are presented in Table 1.

Procedure: the experiments were adjusted at initial pH of 5.5 for Pb(II) and 5.4 for Cu(II) which was determined experimentally. The pH values were adjusted with 0.1M NaOH and 0.1M HCl.

The fixed bed experiments were carried out in Perspex glass column of 38.1mm (I.D.) and 40 cm in height with perforated support at the bottom of the column to support the activated carbon bed and distributer at the top of the column. Bed height in packed bed is controlled with packed mass of carbon. Plastic beads with depth 3 cm were placed at the top of the activated carbon bed to ensure a uniform distribution of the influent through the carbon bed. Feed tank of 2 liters was used, which is placed at the top of the adsorber. Feed solution were prepared in feed tank and introduced to the column through the distributor.

For the determination of adsorption isotherm, a volume of 10 ml of metal ion solution in different initial concentration of 10-200 mg/L was placed in ten test tubes containing the fixed mass of activated carbon (0.1 and 0.2g of activated carbon were used for Pb(II) and Cu(II) respectively). The test tubes were then shaken at a constant speed of 250 r.p.m. in a shaking water bath at 25°C ± 1 for 24 hrs. . After shaking the activated carbon was separated by centrifuge and filtration through a membrane filter 0.45µm. The filtrate was analyzed for the remaining metal ion concentration by atomic absorption spectrometer AAS. The adsorbed amount is calculated by the following equations:

$$q_e = \frac{V}{W}(C_o - C_e) \quad \text{....(25)}$$

$$q_e = f(C_e) \quad \text{.....(26)}$$

The pore diffusion coefficient for each solute was obtained by 1L Pyrex beaker fitted with a variable speed mixer. The beaker was filled with 0.5L of known concentration solution and the agitation started before adding GAC. At time zero , the calculated weight of activated carbon was added, then the samples were taken at every 5 min.

The weight of activated carbon used to reach equilibrium related concentration of C_o/C_e equal 0.05 is calculated from isotherms model and mass balance equation.

4. Results and Discussion

4.1. Adsorption Isotherm. The adsorption isotherm curves were obtained by plotting the weight of the solute adsorbed per unit weight of the adsorbent (q_e) against the equilibrium concentration of the solute (C_e) [7].

Figs. 1 and 2 show the adsorption isotherm curves for single metal ions Pb(II) and Cu(II) onto activated carbon at 25oC respectively. The experimental data are plotted with the theoretical data obtained from using Langmuir and Freundlich isotherm. It can be seen from Figs. 1 and 2 that the experimental

data follow the Langmuir isotherm model better than the Freundlich isotherm model. In which the Langmuir parameter q_m, b are evaluated to be as follows:

for Pb(II): q_m= 13.333 mg/g, b = 0.312 L/mg
for Cu(II): q_m = 5.845 mg/g, b = 0.710 L/mg

4.2. Pore Diffusion Coefficient. Pore diffusion coefficient D_p for each metal ions are evaluated from the concentration decay curve by matching the experimental data with the predicted data by pore diffusion model for batch adsorber [8] as shown in Figs. 3 and 4. There were a good matching between the batch experimental results and predicted data using pore diffusion model for batch adsorber. The pore diffusion coefficient for each the metal ions are evaluated from batch experiments to be :

For Pb(II): $D_p = 7.955 \times 10^{-10}$ m^2/s
For Cu(II): $D_p = 3.532 \times 10^{-10}$ m^2/s

The amount of GAC used for each metal ions were calculated for final equilibrium related concentration of C_e/C_o = 0.05, using the Langmuir isotherm with mass balance in one liter of solution. The initial concentration were 0.06 and 0.1kg/m^3 with the doses of activated carbon of 0.01 and 0.02 Kg for Pb(II) and Cu(II) respectively.

The external mass transfer coefficient in packed bed column model was calculated used the correlation of Wilson and Geankoplis [9]. The molecular diffusion coefficient D_m used is 1.43×10^{-9} m^2/s [10].

$$Sh = \frac{1.09}{e_b} \mathrm{Re}^{1/3} Sc^{1/3} \text{ for } 0.0015 < \mathrm{Re} < 55 \quad \ldots.(27)$$

Where $Sh = k_f d_p / D_m$

$$Sc = m_w / r_w D_m ,$$

$$\mathrm{Re} = r_w n d_p / m_w$$

These values substituted in equation 27 to evaluated k_f at different interstitial velocity in the mathematical model. The axial dispersion coefficient calculated from Chung and Wen equation [11] :

$$\frac{nL}{D_L} = \frac{L}{2 R_p e_b} \left(0.2 + 0.011 \, \mathrm{Re}^{0.48}\right) \quad \ldots.(28)$$

4.3. Breakthrough Curve. Figs. 5 and 6 show the experimental and predicted breakthrough curves for Pb(II) and Cu(II) respectively obtained for different flow rates in terms C_e/C_o versus time. It is clear from the these figures that as the flow rate increases the time of breakthrough point decreases. This is because the residence time of solute in the bed decreases as the flow rate increases and therefore there is not enough time for adsorption equilibrium to be reached which results in lower bed utilization and the adsorbate solution leaves the column before equilibrium.

It is expected that the change in flow rate will affect the film diffusion but

not the intraparticle diffusion. The higher the flow rate the smaller the film resistance to mass transfer and larger k_f result.

Increasing flow rate at constant bed height will increase the Biot number with slight increases in Peclet number as listed in Table 2 . Biot number is defined as the ratio of the external mass transfer to intraparticle mass transfer. When the Biot number is high the time of breakthrough point will appear early. The higher Biot number value indicates that the film diffusion is not a dominating compared to the intraparticle mass transfer and the intraparticle mass transfer is the controlling step. These results are in agreement with that obtained by [5,6,10,12,13,14 and 16].

The bed depth is one of the major parameters in the design of fixed bed adsorption column. The effect of bed height on the breakthrough curve was studied for Pb(II) and Cu(II) respectively for adsorption onto activated carbon. The experimental and predicted breakthrough curves obtained for different bed height of activated carbon at constant flow rate and constant concentration of metal ion are presented in Figs. 7 and 8. It is clear from these figures that at smaller bed height the effluent metal ion concentration ratio increases more rapidly than at a higher bed height. Furthermore at smaller bed height the bed is saturated in less time compared with the higher bed height. Smaller bed height means lesser amount of activated carbon than for the higher one. Peclet number, Pe, is defined as the ratio of the axial convection rate to the axial dispersion rate. An increase in bed height at constant flow rate will increase the Peclet number with constant Biot number as listed in Table 3. When the Peclet number is small the effect of axial dispersion is not negligible and the break point appears early and the breakthrough point increases with increasing the Peclet number. Hence, the internal and external resistances are confirmed to be the main parameters that control the adsorption kinetics with the increases in the bed height. It is clear that increasing the bed height increases the breakthrough time and increases the residence time of the metal ion solution in the bed. These results are in agreement with that obtained by [5,6,12,13 and 14].

The effect of initial metal ion concentration on the breakthrough curves for each metal ions was investigated for all the systems. The change in initial metal ion concentration will have a significant effect on the breakthrough curves. Figs. 9 and 10 show the experimental and predicted breakthrough curves at different initial metal ion concentrations. These figures show that as the initial metal ion concentration increases the time of breakthrough point decreases. The high initial ion concentration the faster the breakthrough, however the activated carbon loadings are larger at higher initial metal ion concentration. For high initial metal ion concentration, steeper breakthrough curves are found because the equilibrium is attained faster for

higher initial metal ion concentration, which would be anticipated with the basic increase in the driving force for mass transfer with increase in initial metal ion concentration. Similar findings have been obtained by [6,10,12,13,14,15 and 16].

Nomenclature:

b	Adsorption equilibrium constant, m^2/s
Bi	Biot No. $(k_f R_p / e_p D_p)$
C	Fluid phase concentration, kg/m^3
C_e	Equilibrium liquid phase concentration, kg/m^3
C_o	Initial liquid-phase concentration, kg/m^3
D_L	Axial dispersion coefficient, m^2/s
D_m	Molecular diffusivity, m^2/s
D_p	Pore diffusion coefficient, m^2/s
d_p	Particle diameter, m
K_f	Constant in Freundlich
k_f	External mass transfer coefficient, m/s
L	Length of the column, m
n	Constant in Freundlich equation
Pe	Peclet Number, $(nL/D_L$
Q	Fluid flow rate, m^3/s
q_e	Adsorption capacity at equilibrium, kg/kg
q_m	Langmuir constant, kg/kg
r	Radial coordinate, m
R	Radial Coordinate, m
R_p	Radius of particle, m
Sc	Schmidt number, $Sc = m_w / r_w D_m$
Sh	Sherwood number, $Sh = k_f d_p / D_m$
t	Time, s
V	Volume of the solution, m^2
W	Mass of granular activated carbon, kg
Z	Axial distance, m
ε_b	Bed porosity
ε_p	Porosity of adsorbent
ν	Interstitial velocity, $(Q/pR_p^2 e_b)$, m/s
μ_w	Viscosity of water, Pa.s
ρ_w	Density of water, kg/m^3
ρ_p	Particle density, kg/m^3

subscript

b	Bulk fluid phase
e	Equilibrium
GAC	Granular activated carbon
L	Liquid phase
o	Initial
p	Particle phase

Conclusions

1. A film-pore diffusion model has successfully used to describe the adsorption process and to predict the breakthrough curve for single system adsorption of lead and copper in fixed bed adsorber.
2. The equilibrium isotherm curve for adsorption of lead and copper in batch adsorber is of favorable type and the Langmuir isotherm model gives the best fit to the experimental data in comparison to the other isotherm model.
3. In batch adsorber the pore diffusion model has been successfully used to estimate the pore diffusion coefficient by matching between the experimental and theoretical concentration decay curves. This model gives a good maching.
4. The time of the breakthrough point decreases with the increase in flow rate, increases initial metal ion concentration and decreases in bed height.

References

[1] Aslam, M.M., Hassan, I., Malik, M. and Matin, A., 2004, "Removal of Copper from Industrial Effluent by Adsorption with Economical VariableMaterial", Electronic J. of

Environment, Agriculture and Food Chemistry EJEAFChe, 3 (2),pp.658-664.

[2] WHO, 1984, World Health Organization, Geneva Guidelines for Drinking Water Quality, 1984.

[3] IPCS, 1988, International Programme on Chemical Safty Environmental Health Criteria World Health Organization Geneva.

[4] Liao, H.T and Shian, C.Y.,2000, "Analytical solution to an Axial Dispersion Model for the Fixed-Bed Adsorber", AIChE J., 46(6), pp.1168-1176.

[5] Babu, B.V. and Gupta, S., 2005, "Modeling and Simulation of Fixed Bed Adsorption Column: Effect of Velocity Variation", J. Eng. Tech., 1, pp. 60-66.

[6] Sulaymon, A.H., and Ahmed, K.W., 2008, "Competitive Adsorption of Furfural and Phenolic Compound onto Activated Carbon in Fixed Bed Column", Environ. Sci. Technol. 42(2), pp.392-397.

[7] Ho, Y.S., Porter, J.F. and McKay, G., 2002, "Equilibrium Isotherm Studies for the Sorption of Divalent Metal Ions onto Peat: Copper, Nickel and Lead single Component Systems", Water, Air and Soil Pollution, 141, pp. 1-33.

[8] Al-Najar J. A., 2009, "Removal of Heavy Metals by Adsorption Using Activated Carbon and Kaolinite" Ph.D. Thesis, University of Technology, Baghdad, Iraq.

[9] Wilson, E.j. and Geankoplis, C.J., 1966, "Liquid Mass Transfer at very Low Reynolds Number in Packed Bed", Ind. Eng. Chem. Funda., 5(1), pp. 9-12.

[10] Ko, D.C.K., Porter, J. F. and McKay, G., 2001, "Film-Pore Diffusion Model for the Fixed-Bed Sorption of Copper and Cadmium Ions onto Bone Char", Wat. Res., 35(16), pp.3876-3886.

[11] Hang, T., 2003, "Ion Exchange Modeling of Crystalline Silicotitanate Column from Cesium Removal from Argentine Waste(U)", Wisting House Savannah River Company.

[12] Wong, K.K., Lee, C.K., Low, K.S. and Haron, M.J. 2003, "Removal of Cu and Pb from Electroplating Wastewater Using Tartaric Acid Modified Rice Hisk", Process Biochemistry, 39, pp.437-445.

[13] Ahmed, K.W., 2006, "Removal of Multi-pollutants from Wastewater by Adsorption Method ", Ph.D. Thesis, University of Baghdad.

[14] Ebrahim, S.E., 2008, "Evaluation of a Mixture Adsorbent and Glass Bead for the Removal of Phenol and Methylene Blue from Water", Ph.D. thasis, University of Baghdad.

[15] Reed, B.E., Arunachalam, S. and Thomas, B., 1994, "Removal of Lead and Cadmium from Aqueous Stream Using Granular Activated Carbon", Environ. Progr., 13(1), pp.60-64.

[16] Smith, E.H. and Amini, A., 2000, " Lead Removal in Fixed Beds By Recycled Iron Material", J. Environ. Eng., 12(1), pp.58-65.

Table 1, Physical properties of granular activated carbon

Product name	Activated carbon, DARACO 20-40 mesh,
Company	Sigma-Aldrich Company (UK) Ltd
Composition	Carbon C
Bulk density, kg/m^3	336
BET surface area, m^2/g	602.97
Average pore diameter,	3.72
pH	6-9

Table 2. The values of Biot No. and Peclet No. at different flow rates.

Metal ions	Flow rate, Q	Biot No.	Peclet
Pb(II)	0.667x10^{-6}	41.54	35.06
	1.000x10^{-6}	47.54	35.43
	1.330x10^{-6}	52.32	35.74
Cu(II)	0.667x10^{-6}	93.56	35.06
	1.000x10-6	107.08	35.43
	1.330x10^{-6}	117.84	35.74

Table 3., The values of Biot No. and Peclet No. at different bed heights.

Metal	Bed height,	Biot No.	Peclet No.
Pb(II)	0.05	41.54	17.53
	0.10	41.54	35.06
	0.20	41.54	70.11
Cu(II)	0.10	107.08	35.43
	0.15	107.08	53.14
	0.20	107.08	70.85

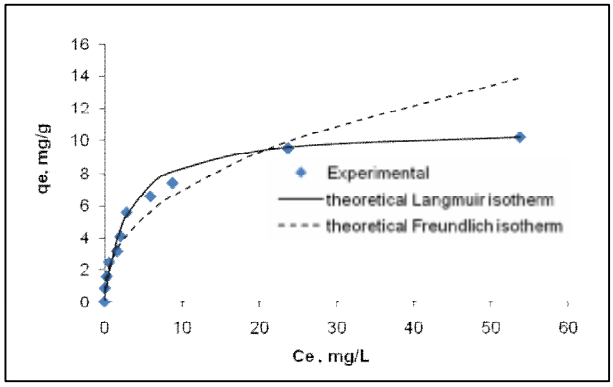

Fig.1, Adsorption isotherm for Pb(II) onto activated carbon (0.1 g activated carbon, Temp. = 25°C)

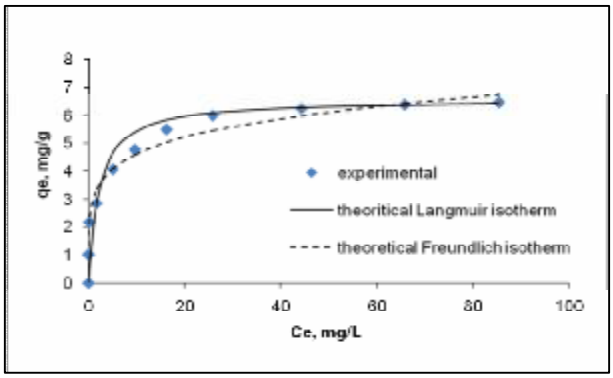

Fig.2, Adsorption isotherm for Cu(II) onto activated carbon (0.2 g activated carbon, Temp. = 25°C)

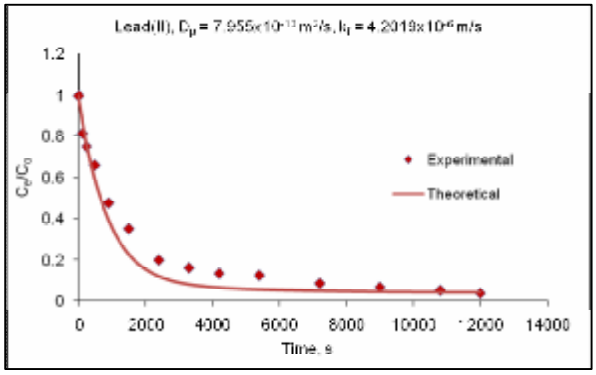

Fig.3, Comparison of the measured concentration-time decay data with that predicted by pore diffusion model for Pb(II) in batch adsorber

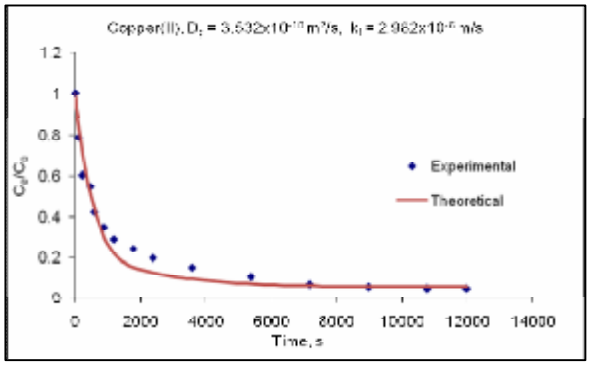

Fig.4, Comparison of the measured concentration-time decay data with that predicted by pore diffusion model for Cu(II) in batch adsorber

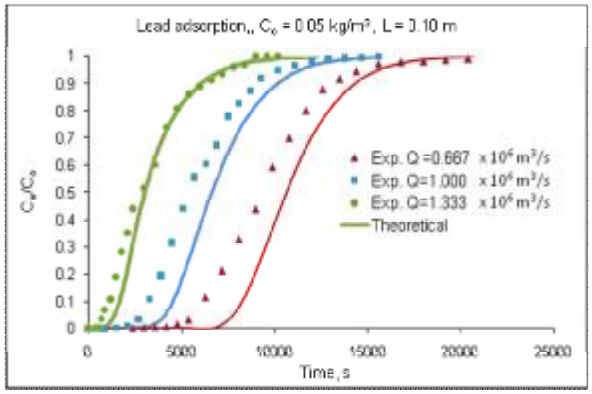

Fig.5, The experimental and predicted breakthrough curves for adsorption of Pb(II) onto activated carbon at different flow rates.

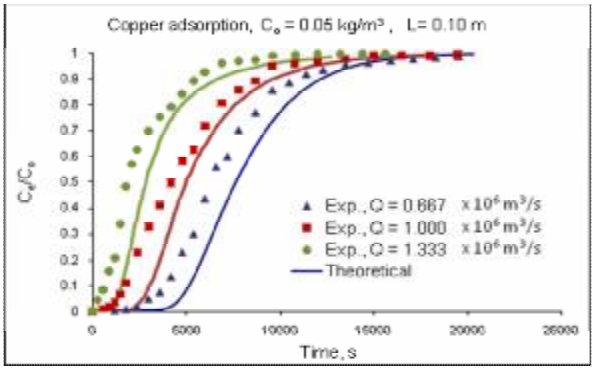

Fig.6, The experimental and predicted breakthrough curves for adsorption of Cu(II) onto activated carbon at different flow rates

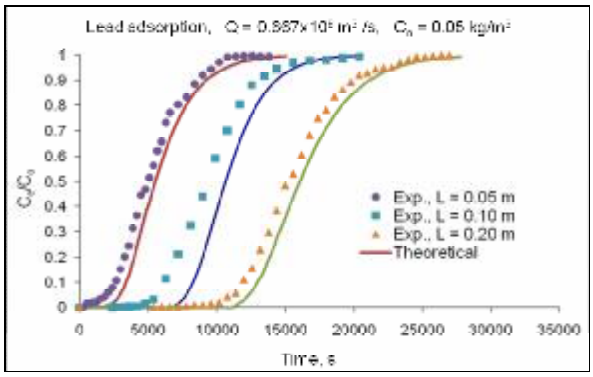

Fig.7, The experimental and predicted breakthrough curves for adsorption of Pb(II) onto activated carbon at different bed heights.

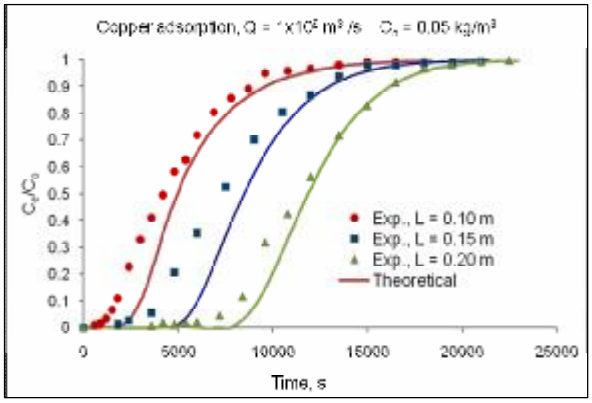

Fig.8, The experimental and predicted breakthrough curves for adsorption of Cu(II) onto activated carbon at different bed heights.

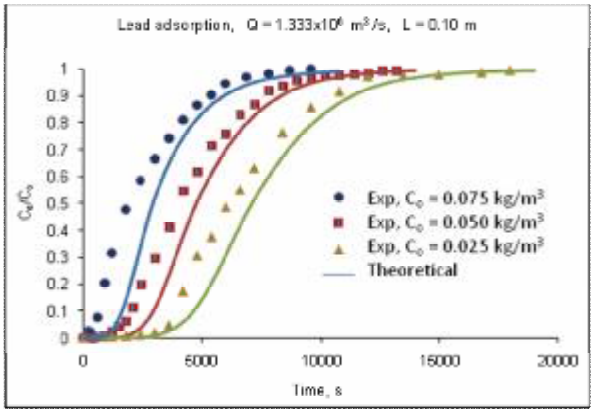

Fig.9, The experimental and predicted breakthrough curves for adsorption of Pb(II) onto activated carbon at different initial metal ion concentrations

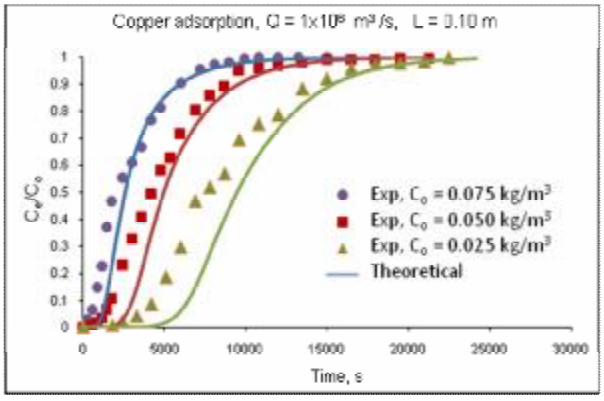

Fig.10,The experimental and predicted breakthrough curves for adsorption of Cu(II) onto activated carbon at different initial metal ion concentrations.